

Fatigue analysis of brittle materials using indentation flaws

Part 2 Case study on a glass-ceramic

R. R. COOK, B. R. LAWN*, G. R. ANSTIS†

Department of Applied Physics, School of Physics, University of New South Wales, Kensington, NSW 2033, Australia

The results of an experimental dynamic fatigue study on glass-ceramic specimens containing indentation flaws are analysed in terms of the theory developed in Part 1. A Vickers indenter is used to introduce the flaws, and a conventional four-point bend apparatus to break the specimens. Base-line data for testing the essential theoretical predictions and for evaluating key material/environment parameters are obtained from "polished" surfaces, i.e. surfaces prepared to a sufficient finish to ensure removal of any pre-existing spurious stresses. The fatigue tests are carried out in water. Inert strength tests in dry nitrogen are used to "calibrate" appropriate equilibrium fracture parameters, with "dummy" indentations on selected control specimens providing a convenient measure of the critical crack dimensions at failure. Regression analysis of the dynamic fatigue data yields values for "apparent" kinetic parameters, which are converted to "true" kinetic parameters via the transformation equations of Part I. Regeneration of the fatigue function from the theory using the parameters thus determined gives a curve which passes closely through the experimental data points, thereby providing a self-consistent check of the formalism. The implications of the results in relation to the use of macroscopic fracture parameters in the prediction of strength properties for materials with small-scale flaws is an important adjunct to this work. Finally, a recommended procedure for the general testing of dynamic fatigue properties of ceramics using indentation flaws is described.

1. Introduction

In Part 1 of this study [1] we outlined the theoretical framework for evaluating fatigue parameters from tests on as-indented strength specimens. Emphasis was placed on accommodating a residual contact component explicitly into a general fracture mechanics formulation, such as to ensure optimal simplicity and economy in the experimental test programme. Our aim in this paper is to demonstrate, by way of a case study, the practical application of the method.

Accordingly, results are presented here for dynamic fatigue tests on a magnesium aluminosilicate glass-ceramic (Pyroceram C9606, manufactured by Corning Co.) in water. This choice of a "typical ceramic" derives from three considerations: firstly, independent investigations of the fracture properties have been made by other workers; secondly, it is known (from these independent investigations) that the susceptibility to fatigue (as measured inversely by the crack velocity exponent n) is not high, so the sensitivity of the method should be clearly illustrated; third, the material has a reasonably fine microstructure, which is conducive to the production of "well-behaved" radial-crack patterns. A routine two-

silicate glass-ceramic (Pyroceram C9606, manufactured by Corning Co.) in water. This choice of a "typical ceramic" derives from three considerations: firstly, independent investigations of the fracture properties have been made by other workers; secondly, it is known (from these independent investigations) that the susceptibility to fatigue (as measured inversely by the crack velocity exponent n) is not high, so the sensitivity of the method should be clearly illustrated; third, the material has a reasonably fine microstructure, which is conducive to the production of "well-behaved" radial-crack patterns. A routine two-

*Present address: Fracture and Deformation Division, National Bureau of Standards, Washington, D.C. 20234, USA.

†Present address: Department of Metallurgy and Science of Materials, University of Oxford, Oxford, UK.

step procedure, indentation by a Vickers diamond pyramid followed by constant-rate flexure to failure, is used to obtain the basic strength data. Requisite values of the critical crack dimensions are obtained by a contrived experiment whereby control specimens containing “dummy” indentations are subjected to post-failure microscopic examination. The theory developed in Part 1 is then used to evaluate the pertinent fracture parameters for the material.

In the course of the analysis due emphasis will be placed on the key role of the residual contact stresses in the fracture mechanics to failure. In addition, attention will be paid to some of the “secondary” effects dealt with in Part 1, e.g. those relating to the surface stress state *prior* to indentation and a multi-region crack velocity function, which are found to have an important bearing on the fatigue response.

2. Test procedure

2.1. Preparation and indentation of glass-ceramic specimens for strength testing

Pyroceram C9606 is a magnesium aluminosilicate glass-ceramic, with cordierite ($2\text{MgO} \cdot 2\text{Al}_2\text{O}_3 \cdot 5\text{SiO}_2$) the main crystalline phase. Some minor crystalline phases are also present, among them titania (TiO_2) which is included as a nucleating agent, and $\approx 5\%$ glassy phases. The material has a microstructure in the size range of 1 to $10\ \mu\text{m}$, but can contain pores of a somewhat larger dimension. More detailed descriptions of the microstructure in relation to strength properties are to be found elsewhere [2, 3].

Specimens suitable for bend testing were supplied to us by B. J. Pletka and S. M. Wiederhorn* in the form of bars 32 mm by 6 mm by 4 mm. These bars were cut from the same billet of material used by Pletka and Wiederhorn in their comparative study of the macroscopic crack growth and fatigue properties of Pyroceram [3, 4]. The surfaces of the bars had all been machined with a 400-grit diamond wheel. Approximately one half of the specimens were given a further surface finish on their prospective tensile faces, using a slurry of 1000-grit SiC to remove a layer $> 100\ \mu\text{m}$; this was done in accordance with a preliminary investigation into the effects of surface state on strength [5], where it was demonstrated that a finish of this kind is effective in removing significant residual stresses due to

the relatively severe machining-damage treatment. Of these “polished” specimens, a few were smoothed to a final mirror surface finish with $1\ \mu\text{m}$ diamond paste, to provide optimal reflectivity for ensuing crack observation.

Each bar was then indented with a Vickers diamond pyramid at the centre of its prospective tensile face at a standardized tensile load, $P = 20\ \text{N}$. This load was selected on the basis of crack-size considerations: on the one hand, the crack should be sufficiently large in comparison with the microstructure and with the scale of the central deformation zone that it may be considered to be “well-developed”; on the other, the crack should always remain small relative to the specimen dimensions. The Vickers pyramid was oriented to produce radial crack traces parallel to the specimen edges. All indentations were made in air, at a fixed load duration of 10 sec. Those specimens prepared with mirror-smooth surfaces were given a special indentation treatment: additional indentations were made along the longitudinal centre-line in the tensile face, giving a total of three within the inner-span region and one in the outer overhang region of the test bar, with each spaced at least 1.5 mm from its neighbours and from the specimen supports (see below) to avoid interaction effects. All indented specimens were allowed to sit for approximately 1 h, in air, before strength testing.

The specimens thus prepared were then broken in four-point flexure, with an inner span of 7.5 mm and an outer span of 24.0 mm. A cross-head testing machine was used to deliver the bending load, which was monitored by two load cells: a conventional strain-gauge instrumented load cell was used for “slow” tests, corresponding to failure times > 1 to 10 sec; for “fast” tests, a piezoelectric cell with a frequency response of 60 kHz, was switched in. Simple beam theory was used to evaluate the stress in the tensile surface. Both cells gave a linear stress–time response at constant cross-head speed; a working range of stress rates of $\dot{\sigma}_a \approx 2.5 \times 10^{-3}$ to $2.5 \times 10^3\ \text{MPa sec}^{-1}$ was available to us with this composite system. The test environment during flexure to failure was controlled in accordance with the special requirements of the strength property under examination, i.e. inert or fatigue strength, as described in the subsections below. All broken test-pieces were examined routinely by optical microscopy to

*Fracture and Deformation Division, National Bureau of Standards, Washington, D.C. 20234, USA

TABLE I Strengths of indented bars

Number of bars	Finish	Environment	Strength (MPa)
14	1000-grit SiC	Air	$145 \pm 7^\dagger$
11	1 μm diamond	Dry argon*	147 ± 5

*The bars were placed inside plastic envelopes to confine the gas flow.

† The errors represented standard deviations.

confirm that failure had indeed initiated from the indentation site.

2.2. Inert strength parameters

In the theoretical analysis in Part 1 it was demonstrated that the parameters σ_m and c_m , representing the stress and dimension at the unstable equilibrium configuration for radial cracks driven by applied tensile loading in combination with residual-contact forces, afford a most convenient base for data reduction. This configuration obtains at failure under "inert" environmental conditions, i.e. such that kinetic crack growth effects of the type embodied in the crack-velocity expression Equation 4 of [1] are entirely absent. Accordingly, strength tests were run on the polished, as-indented bars at the fastest available stress rate (2.5 GPa sec^{-1}), the results are shown in Table I. Since these results show no measurable dependence on the environment we may assume (subject to confirmation of the precursor-crack-growth proviso, below) that they correspond closely to true inert strengths, i.e. $\sigma_m = \sigma_i = 146 \pm 6$ MPa (25 combined tests)*. (In this context, it may be noted that similar tests on as-indented soda-lime glass at a stress rate some three orders of magnitude lower than that used here produced indistinguishable strength results in dry nitrogen and vacuum environments [6].) The present tests also indicate that the surface finish, if sufficiently smooth, is not a critical factor; moreover, recalling that the diamond-finished surfaces contained three indentations within the tensile span, it is seen that (at least for the Pyroceram specimens used in our tests) the inert strength is not sensitive to the "multiplicity" of radial cracks.

For the determination of the crack-size parameter, c_m , a post-failure examination was made of the surviving indentations on the diamond-finished surfaces. The frequency of failure was found to be approximately the same for the central as for each of the two flanking indentations

within the inner span, as would be expected for non-interacting crack systems within a uniform tensile field. Thus for any given specimen it can be argued that the two surviving indentations from within this inner tensile region must themselves have been on the verge of instability, thus providing us with intact, dummy crack systems for evaluating critical crack dimensions. In this interpretation, those arms of the radial crack systems aligned *perpendicular* to the tensile direction should give a direct measure of c_m ; those arms *parallel* to the tension should similarly give a measure of c'_0 , the crack size prior to strength testing. Fig. 1 is a representative example of the fracture asymmetry observed in a typical dummy system. Actual crack measurements were made by optical microscopy. Owing to the poor crack visibility in the Pyroceram surfaces special care had to be taken to optimize optical conditions, e.g. by flash coating the specimens with gold and using interference contrast at high power ($\times 700$). The values obtained in this way were $c_m = 98 \pm 15 \mu\text{m}$ and $c'_0 = 69 \pm 13 \mu\text{m}$ (22 indentations). By way of reinforcement of the latter determination, measurements were also made of the crack dimensions for those indentations placed in the stress-free, overhang regions of the bend specimens; these measurements, averaged over the four arms of the radial crack system at each indentation, gave $c'_0 = 63 \pm 7 \mu\text{m}$ (11 indentations). The results confirm that the above-mentioned precursor-crack-growth proviso, $c'_0 < c_m$, is satisfied in this material.

Inert strength tests were also run on bars with original machined surfaces, both with and without indentations. For bars with indentations, we obtained $\sigma_i = 212 \pm 12$ MPa (14 bars). This value is some 45% greater than that obtained for polished surfaces with ostensibly identical indentations, reflecting the substantial level of residual compressive stress that can be introduced by heavy machining damage [5]. For machined bars without indentations, the tests gave $\sigma_i = 273 \pm 9$ MPa (10 bars). This result demonstrates that the indentation flaws, while sufficiently large to constitute dominant failure centres in all out tests, are only slightly more severe than the machining flaws.

2.3. Dynamic fatigue tests

For the dynamic fatigue tests proper, the indentation site on each bar was covered with a drop of

*All errors in this paper are standard deviations about the mean, unless specified otherwise.

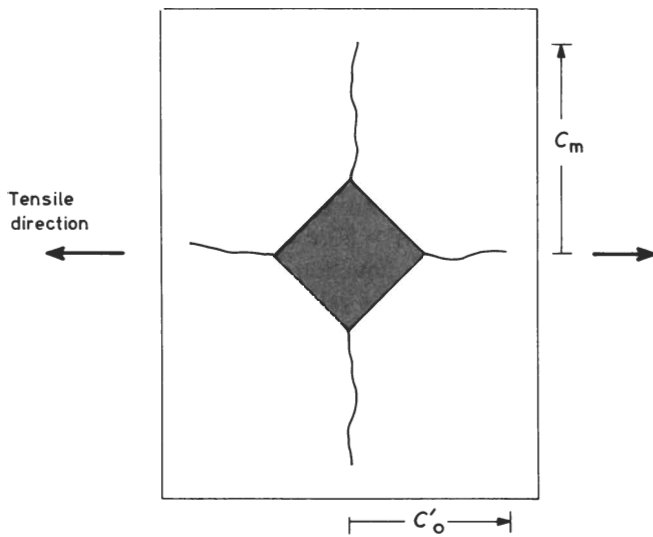


Figure 1 Representation of the radial crack pattern at a dummy indentation in Pyroceram glass-ceramic.

distilled water immediately prior to mounting the bar onto the bending fixture. A glass cover slip was placed over the freshly applied drop to inhibit evaporation during subsequent testing; adhesive tape wound around the covered indentation helped to maintain the specimen intact after failure. For the 1000-grit-polished, as-indented surfaces, an average of 10 bars were broken at each predetermined stress rate. The results are plotted in the conventional manner for dynamic fatigue data, i.e. as $\log \sigma$ against $\log \dot{\sigma}_a$, in Fig. 2. This plot becomes our basis for analysing the intrinsic kinetic fracture response of Pyroceram glass ceramic in water environment, in terms of the theory presented in Part 1 (see Section 3, below). It is immediately evident from the data

points that the material is susceptible to fatigue, even at the fastest stress rate (which corresponds to a test duration of approximately 50 msec), with a near-linear relation between the logarithmic co-ordinates over the range of stress rates covered.

Comparative test runs were made for the machined, as-indented surfaces to investigate the effect of a pre-indentation surface stress state on fatigue properties. The results of these tests are plotted in Fig. 3, together with the data from Fig. 2 for the polished, similarly-indented surfaces, and from the study of Pletka and Wiederhorn [4] for machined surfaces without indentations. Notwithstanding a greater scatter in individual data points, the machined surfaces show fatigue characteristics distinctly different from those of

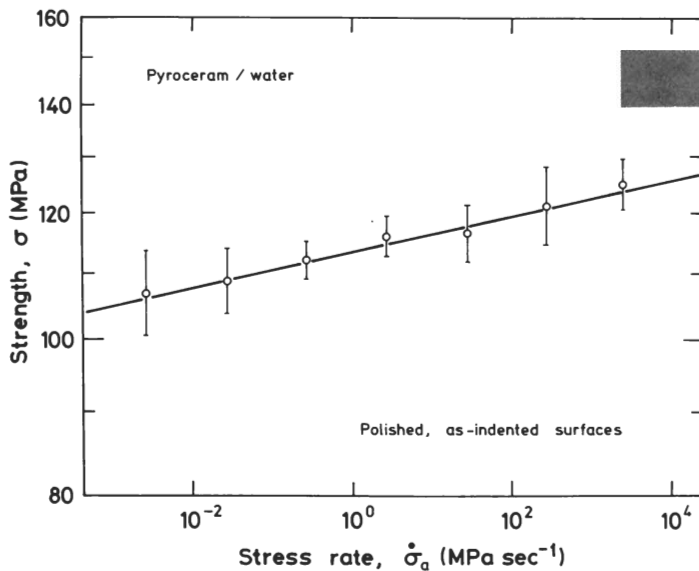


Figure 2 Dynamic fatigue response of Pyroceram glass-ceramic in water, for polished surfaces indented at $P = 20$ N. The shaded band indicates the inert strength level. The degree of fit between the theoretically generated solid curve (using calibrated fracture parameters from inert and fatigue strengths) and the data points may be taken as a measure of the validity of the residual-stress basis of the indentation analysis.

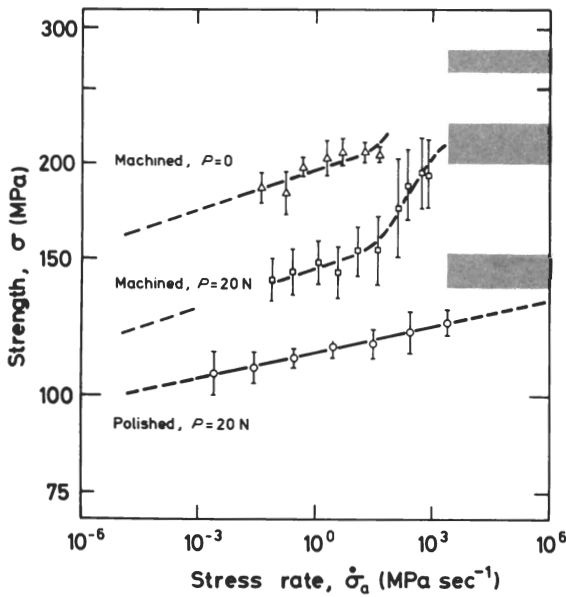


Figure 3 Dynamic fatigue response of Pyroceram glass-ceramic in water, for various surface preparations: polished, as-indentured (reproduced from Fig. 2); machined, as-indentured; machined surfaces without indentations (reproduced from the study by Pletka and Weiderhorn, [4]). The shaded bands are appropriate inert strength levels. The upper two curves in this plot are approximate fits through the data.

the polished surfaces, most noticeably in the departure from linearity at high stress rates for the as-indentured surfaces and in the slopes of the curves in the "linear" region.

3. Analysis of dynamic fatigue data

Let us now consider the results of the previous Section in terms of the theory outlined in Part 1 [1]. The data in Fig. 2 for polished, as-indentured surfaces are taken as our reference base. The apparent linearity in these data makes for relatively straightforward analysis, indicating as it does an absence of complication from pre-indentation surface stresses and multi-region crack velocity functions. Accordingly, the solid curve in Fig. 2 is a theoretical fit of Equation 5 of [1], evaluated from the combined inert and fatigue strength data as follows:

(a) Taking the inert strength parameters $\sigma_m = 146 \pm 6$ MPa and $c_m = 98 \pm 15$ μm from Section 2.2, the composite equilibrium quantities K_c/χ_r and $K_c/(\pi\Omega)^{1/2}$ are evaluated as 83 ± 20 and 1.93 ± 0.20 MPa $\text{m}^{1/2}$ respectively from Equation 3 in [1].

(b) From a linear regression analysis of $\log \sigma$

against $\log \dot{\sigma}_a$ for the fatigue strength data represented in Fig. 2 (but using individual points rather than mean values) values of the slope, $1/(n' + 1) = 0.0112 \pm 0.0013$ and intercept, $(\log \lambda')/(n' + 1) = 2.055 \pm 0.003$ (expressed in terms of the units displayed on the axes in Fig. 2) are obtained as per Equation 2, from which the "apparent" kinetic parameters $n' = 89 \pm 10$ and $\log \lambda' = 184 \pm 20$ follow. Then Equation 14 of [1] is used in conjunction with the values of σ_m and c_m , to evaluate "true" kinetic parameters $n = 116 \pm 13$ and $\log (\nu_0/m \text{ sec}^{-1}) = 5.0$. (All errors quoted in this paragraph are standard errors.)

(c) Now the dynamic fatigue curve is determined from Equation 5 of [1] by solving numerically to obtain the failure stress, σ , for specified values of stress rate $\dot{\sigma}_a$, with an indentation load at $P = 20$ N and an actual measured crack size c_0' of 69 μm as the initial condition.

The quality of fit between the curve thus generated and the data points may be taken as a measure of the validity of the indentation theory. In this context it should be noted that the procedure just outlined involves more than mere curve fitting: in regenerating the fatigue curve we are reliant on the accuracy of the transformation equations for converting kinetic parameters from apparent to true values (these equations themselves embodying several assumptions) and of the calibration of the inert strength parameters. Essentially, the exercise may be seen as a test of the residual-stress hypothesis for contact-induced flaws, in the sense that the key relations used in the parameter evaluations above (namely Equations 3 and 14 of [1]) contain the term χ_r (either explicitly or implicitly) as a vital element in the formulation.

Turning to Fig. 3, we may now attempt to explain the results for the machined surfaces in terms of simple departures from the idealized behaviour of the base-line curve for polished surfaces. Considering first the machined surfaces with indentations, we have already indicated (Section 2.2) that the elevation of strength above the base-line is attributable to the presence of a pre-indentation surface compressive stress layer. However, such a compressive stress cannot be acting uniformly over the entire indentation-crack area, for, if it were, according to Fig. 7 of [1], the fatigue plot would tend to a non-linear curve with reduced slope in the low stress-rate region; if anything, the curve for machined surfaces tends